Tellus (1983), *35A*, 363–378

The use of dynamical constraints in the analysis of mesoscale rawinsonde data

By STEPHEN C. BLOOM, *Laboratory for Atmospheric Research, University of Illinois, Urbana, Illinois 61801, U.S.A.*[1]

(Manuscript received June 9, 1982; in final form January 4, 1983)

ABSTRACT

This study seeks to generate dynamically consistent analyses of mesoscale rawinsonde data by coupling analyses of winds and geopotentials on pressure surfaces. The approach used here follows in a general way the one taken by Lewis and Bloom (1978) in their analysis of surface data; the observations are first objectively analyzed onto a regular grid in space and time, and the gridded fields are then adjusted in a least-squares sense using a set of forecast equations of horizonatal momentum as dynamical constraints. However, the scheme described in this paper has a more consistent treatment of the adjustments to the fields in time. The adjustment process is tested on objectively analyzed rawinsonde soundings from two cases from the data archives of the National Severe Storms Laboratory (NSSL); 8 June 1966 and 22 May 1966. The principal results of this study are: (1) the initial winds and geopotentials produce unphysical residuals when they are put into the momentum constraints; (2) the adjusted fields have greatly reduced residuals, (3) the adjustments to the wind and geopotential fields have root-mean-square values of 1–2 m s^{-1} and 30–50 m^2 s^{-2} respectively, and (4) the vertical velocity fields computed from the adjusted winds are more consistent with the weather events that occurred in the two data cases.

1. Introduction

The processing of irregularly distributed meteorological observations, whether for use in research analyses or in forecast models, must entail the interpolation of data to some form of regular grid in space and time. Such interpolation procedures degrade the usefulness of the processed fields by introducing mutual inconsistencies among the variables.

A previous study, Lewis and Bloom (1978), hereafter referred to as LB, examined an analysis process which incorporated dynamical consistency into subsynoptic surface analyses. The major motivation behind that research was the examination of the effect of improved time continuity of map analysis upon the behaviour of the surface convergence fields. They found that their scheme improved both the depiction of the development of surface convergence and the correlation between the surface convergence patterns and the observed radar echoes.

This study applies the basic analysis philosophy of LB to a different type of data: mesoscale rawinsonde data obtained from the National Severe Storms Laboratory (NSSL, for a description see Barnes et al., 1971). The difficulties introduced by the interpolation of data to grid points discussed in LB are greatly enhanced in the present analysis by the manner in which the data were sampled. Whereas the distribution of surface data used by LB was fairly dense (with respect to synoptic scales: roughly 110 stations in a $|1600\ \text{km}|^2$ square region), the NSSL rawinsonde data used in this study is very sparse (with respect to mesoscale phenomena: 9 rawinsondes in a |180 km × 240 km| region at any given time). As shown in section 4 of this paper, serious inconsistencies arise as a result of a four-dimensional interpolation of this sparse data to (x, y, p, t) grid points. In an effort to remedy these inconsistencies, a variational adjustment of the interpolated data is developed.

[1] Current affiliation: NASA Goddard Space Flight Center, Code 911, Greenbelt, MD 20771, U.S.A.

The basic method employed in this work follows the general ideas discussed in LB and in a number of papers by Sasaki (1958, 1969, 1970). In principle, the adjustments to the data are minimized in a least squares sense subject to a set of constraints which couple the variables in space and time. Here, as in LB, the horizontal momentum equations are the constraints in the adjustment process. An attempt was made at the start of this work to apply an adaptation of the Thompson (1969) method to multiple pairs of time levels in an iterative manner similar to that in LB. However, it was found that such a scheme was not adequate in this study, since the iterative processes taken from LB did not produce convergent adjustments. The strong temporal and spatial variability of the mesoscale data used here disrupted the iterative procedure. Therefore, a formalism has been developed in this study which can handle a large temporal variability in the data by dispensing with the two-time level approach and developing instead a scheme which treats the temporal variation of the adjustments on an equal basis with the spatial variation of the adjustments. Although the adjustments are applied on "slabs" (x,y,t) in the horizontal and in time, no vertical constraints are applied in this study; i.e. there is a weak coupling in the vertical.

Two cases from the NSSL data archives are used in this work: 8 June 1966 and 22 May 1966. The former is a well-documented (discussed in LB) occurrence of severe storms in the Midwest of the United States, while the latter is an example of a "false-alarm"—a day during which no severe weather occurred in an area which had apparently threatening conditions. In addition to the comparison of observed and adjusted fields, the analyses are also intended to explore the underlying differences between the two cases. A three hour period prior to storm formation in the June case as well as a comparable period in the May case are used to test the adjustment procedure.

2. Development of the adjustment formalism

2.1 *Background and motivation*

The overall analysis procedure in this paper is a two-step process which follows that of LB; a successive-corrections interpolation to gridpoints followed by a variational adjustment. Another approach to the interpolation of the data would be the use of an optimum interpolation scheme (for an example and further references see Schlatter, 1975). However, to use such a technique, one needs both good first-guess fields and reliable models of the first-guess field error statistics; neither were available for the data used in this study. There have been recent advances where the interpolation and adjustment steps have been combined, such as the work of Wahba and Wendelberger (1980); however, such methods appear to become computationally awkward, requiring the inversion of large matrices, if the number of observations becomes large (i.e. $\gtrsim 150$). Although there were only 10 rawinsonde sites in the 1966 NSSL network, the number (N) of observations for each case in this study would be roughly: N = (10 stations) × (3 launches) × (number of significant levels per sounding). Since the final term in N can be as large as 20 or 30, it appears that even the sparse 1966 NSSL data would be unwieldy in a four-dimensional analysis by the combined processes of Wahba and Wendelberger (1980).

The interpolation process used in this paper closely follows the procedure used in Ogura and Chen (1977); it is discussed in detail by Bloom (1980). Briefly, the data, which include the horizontal displacements of the balloons, are interpolated onto a uniform grid in time and pressure using splines under tension (Cline, 1973). Then the data at each pressure-time point are horizontally interpolated with the application of a successive-corrections method with a Cressman (1959) weighting function. The behaviour of this horizontal interpolator was discussed by LB; they found that it behaved mainly as a low-pass filter, and that it should be used to remove wavelengths of the order of the average observation separation or less. The horizontal interpolation of each variable at each pressure-time point is performed independently of all of the other variables and of all the other pressure-time points. This fact has important consequences for the dynamical consistency of the interpolated data. Schaefer and Doswell (1979) have discussed the hazards of interpolating wind components independently; there is a troublesome ambiguity in interpolated vector fields which can be removed by some form of variational adjustment. Further, the separate horizontal interpolations at different times and

pressures would tend to decouple the time and pressure continuity of the different variables. Many of these doubts about the interpolation processes are confirmed by the large momentum budget residuals discussed in section 4.

2.2 *Momentum budgets and constraints*

The hydrostatic, inviscid horizontal equations of motion in pressure coordinates on a tangent plane are:

$$\frac{\partial u}{\partial t} + \mathbf{V}\cdot\nabla u + \omega\frac{\partial u}{\partial p} - fv + \frac{\partial \phi}{\partial x} = 0 \tag{1}$$

$$\frac{\partial v}{\partial t} + \mathbf{V}\cdot\nabla v + \omega\frac{\partial v}{\partial p} + fu + \frac{\partial \phi}{\partial y} = 0 \tag{2}$$

where $\mathbf{V} = (u, v)$ is a horizontal velocity vector and $\nabla = (\partial/\partial x, \partial/\partial y)$ is a horizontal gradient operator. These equations are very similar to the constraints used by LB except for the addition of vertical advection terms and the removal of dissipation terms. By confining the analyses to preconvective or nonconvective periods, and by concentrating on flow properties away from the surface boundary, this study hopes to minimize the inaccuracy of dropping turbulent stress terms from the equations of motion. Unlike the pressures used by LB, which were directly measured, the geopotentials in this study are derived quantities. The geopotentials are computed via a hydrostatic integration of temperatures which have been interpolated to grid points. Fankhauser (1974) has commented on the problems associated with such a procedure: inaccuracies in surface pressures and cumulative integration errors in the vertical, coupled with a small mesoscale spacing can combine to produce large unreliable gradients in the analyzed geopotential. Thus, one can expect the geopotential in this work to be inherently more unreliable than the pressure used in LB.

The vertical velocity, ω, is also a derived quantity. It is computed kinematically by an integration of the horizontal divergence (which in turn is computed from interpolated wind components) with respect to pressure, with an assumption that $\omega = 0$ at 925 mb, the level chosen to be the bottom boundary of the analysis region. Although this is a fairly crude approximation, as it ignores terrain effects, it is consistent with the neglect of boundary-layer processes in the momentum constraints. No condition was assumed for ω at the top of the domain. After the adjustment process, an adjusted ω is computed from the modified winds. Due to its sensitivity to structures in the wind field, comparisons of ω before and after adjustment are used to illuminate the nature of the adjustment process.

Letting E_u and E_v denote the residuals obtained by substituting the interpolated data into eqs. (1) and (2), the momentum budget equations are

$$\frac{\partial \tilde{u}}{\partial t} + \tilde{\mathbf{V}}\cdot\nabla\tilde{u} + \tilde{\omega}\frac{\partial \tilde{u}}{\partial p} - f\tilde{v} + \frac{\partial \tilde{\phi}}{\partial x} = E_u \tag{3}$$

$$\frac{\partial \tilde{v}}{\partial t} + \tilde{\mathbf{V}}\cdot\nabla\tilde{v} + \tilde{\omega}\frac{\partial \tilde{v}}{\partial p} + f\tilde{u} + \frac{\partial \tilde{\phi}}{\partial y} = E_v \tag{4}$$

where a tilde over a variable, $(\sim)$, denotes the original (or previous iteration, see section 3) interpolated data. In the computations of E_u and E_v, the finite difference forms of eqs. (3) and (4) use centered differences with $\Delta t = 15$ min, $\Delta x = \Delta y = 20$ km, $\Delta p = 25$ mb. Note that E_u and E_v are measures of the inconsistencies in the interpolated data with respect to eqs. (1) and (2).

This study seeks to reduce or eliminate E_u and E_v by finding adjustments (u,v,ϕ) so that the adjusted fields

$$\begin{aligned} u_a &= \tilde{u} + u \\ v_a &= \tilde{v} + v \\ \phi_a &= \tilde{\phi} + \phi \end{aligned} \tag{5}$$

satisfy constraints which approximate equations (1) and (2):

$$\frac{\partial u_a}{\partial t} + |\mathbf{V}_a\cdot\nabla u_a|_{\text{prev.}} + \tilde{\omega}\frac{\partial \tilde{u}}{\partial p} - fv_a + \frac{\partial \phi_a}{\partial x} = 0 \tag{6}$$

$$\frac{\partial v_a}{\partial t} + |\mathbf{V}_a\cdot\nabla v_a|_{\text{prev.}} + \tilde{\omega}\frac{\partial \tilde{v}}{\partial p} + fu_a + \frac{\partial \phi_a}{\partial y} = 0 \tag{7}$$

where "prev." denotes the horizontal advection of momentum computed with values of the adjusted winds from a previous iteration (or the observed winds for the first iteration), following a method used by LB—see section 3 of this paper for further details. Note that no attempt was made in this study to incorporate adjustments in the vertical motion field into the vertical advection terms in the momentum constraints. Since this study was confined to pre-convective or non-convective

periods, the vertical advection of momentum was small compared to the other terms in the constraints; thus the neglect of any modifications to the vertical momentum advection in the constraints is justifiable. Note eqs. (3)–(7) can be combined with the adjustments u,v, and ϕ:

$$\frac{\partial u}{\partial t} - fv + \frac{\partial \phi}{\partial x} + E_u = 0 \tag{8}$$

$$\frac{\partial v}{\partial t} + fu + \frac{\partial \phi}{\partial y} + E_v = 0. \tag{9}$$

It should be noted that these constraints differ fundamentally from those used by LB; the time dependence of the variables is no longer treated differently from the spatial dependence. LB treated the time tendency of the variables implicitly by performing adjustments to two adjacent times and then iteratively coupling the results of the sequence of pairs of adjustments. The appearance of explicit time tendency terms in the constraints adds considerable complexity to the adjustment equations; yet now the temporal adjustments of the variables are more consistent.

2.3 *Adjustment equations*

The adjustment variables are obtained by requiring the minimization of a functional I subject to the two momentum constraints; I is given by

$$I = \iiint \left\{ u^2 + v^2 + \gamma\phi^2 + 2\lambda_u \left[\frac{\partial u}{\partial t} - fv + \frac{\partial \phi}{\partial x} + E_u \right] + 2\gamma_v \left[\frac{\partial v}{\partial t} + fu + \frac{\partial \phi}{\partial y} + E_v \right] \right\} \mathrm{d}x\,\mathrm{d}y\,\mathrm{d}t \tag{10}$$

where $\gamma > 0$ is a weighting factor and λ_u and λ_v are Lagrange multipliers. As discussed above, there is some reason to consider the geopotential to be somewhat unreliable; the weighting factor γ allows the adjustment process to incorporate this fact. Using Kurihara (1961) as a guide, one should expect wind errors from rawinsondes to be in the order of 1–2 m s^{-1} (see Table 1). Lenhard (1973) lists the root mean square (RMS) errors in the computed heights of rawinsondes at specified pressures from intercomparison tests (see Table 2). An additional 10 m should be added to those RMS height errors due to the uncertainties in the "base-line" setting of the rawinsondes

Table 1. *Wind speed error in m s^{-1} shown as a function of wind speed and pressure (from Kurihara, 1961)*

	10 m s^{-1}	20 m s^{-1}	30 m s^{-1}
500 mb	1.9	2.0	2.2
700 mb	1.5	1.6	1.7
850 mb	0.6	0.7	0.8

Table 2. *RMS errors in computed heights at specified pressures (from Lenhard, 1973)*

Pressure (mb)	Error (m)
200	11.7
300	8.5
500	4.6
700	2.3

(Fankhauser, 1974). A series of tests established that $\gamma = 0.002$ m^{-2} s^2 gives RMS wind and geopotential adjustments consistent with rawinsonde errors. Instead of a simple constant weight γ, one could have employed three weights for u, v and ϕ, each of which a function of space and time, to give greater influence to those grid points nearest the data (cf. Fig. 1a). However, only the constant γ is kept in this study to simplify eqs. (14)–(15) for the two Lagrange multipliers.

Noting that γ is positive, and that the expressions with the Lagrange multipliers are formally zero, one sees that I is positive definite. The values of $u,v,\phi,\lambda_u,\lambda_v$ which satisfy $\delta I = 0$ (extremum condition) will indeed minimize I if they satisfy appropriate boundary conditions. Performing the first variation of I, one obtains three relations between the adjustment variables and the Lagrange multipliers:

$$u = \frac{\partial \lambda_u}{\partial t} - f\lambda_v \tag{11}$$

$$v = \frac{\partial \lambda_v}{\partial t} + f\lambda_u \tag{12}$$

$$\phi = \frac{1}{\gamma}\left[\frac{\partial \lambda_u}{\partial x} + \frac{\partial \lambda_v}{\partial y} \right]. \tag{13}$$

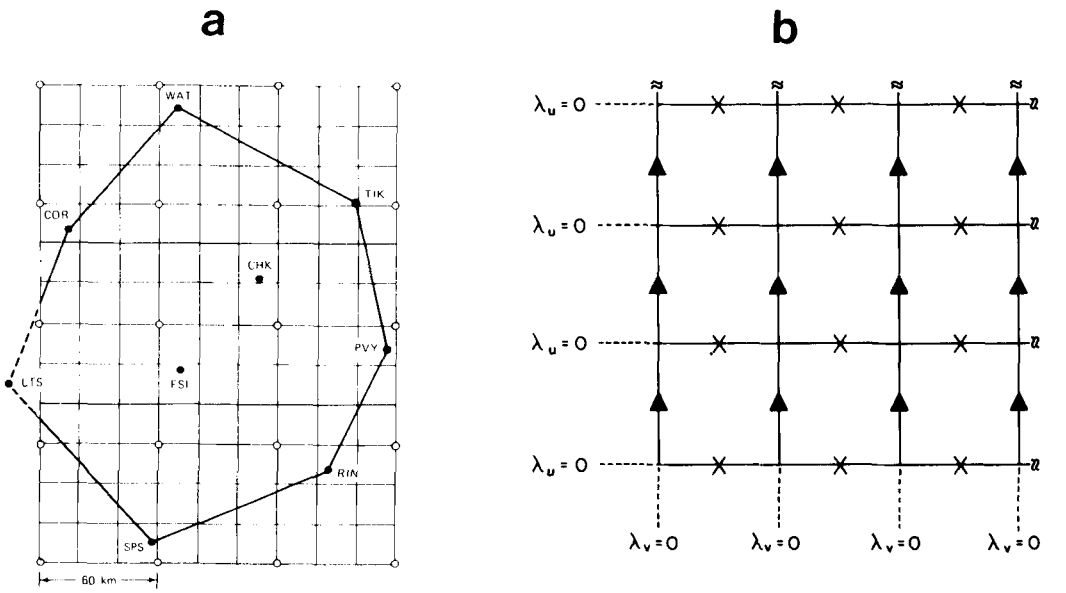

Fig. 1. (a) 1966 NSSL rawinsonde mesonetwork configuration (stations located at solid circles) and the interpolation grid. Details of the analysis process are given in Bloom (1980). (b) Section of the staggered computational grid (lower left-hand corner). Solid lines are the same as those used for the interpolation grid; dashed lines represent boundary conditions for λ_u and λ_v. (U, U, ω, ϕ) are defined at the mesh points; (E_u, λ_u) defined at the "X" points; (E_v, λ_v) defined at the points labelled "Δ".

In arriving at these relations, λ_u is set to zero on x and t boundaries and λ_v is set to zero on y and t boundaries. These conditions cause the boundary integrals to vanish, and assure the minimization of I. Note that the conditions on the time boundaries do allow adjustment to the winds at the bounding times while they hold the geopotentials fixed at those times (i.e. $\phi = 0$ and $u \neq 0$, $v \neq 0$ for initial and final times). This is not an attractive feature of this process since the winds are more trustworthy than the geopotentials. However, an attempt to implement a more realistic adjustment process by setting $u = v = 0$ at the bounding times considerably disrupted the iterative algorithm (see section 3) to the degree that it became non-convergent. Further work is needed on this aspect of the problem.

If eqs. (11)–(13) are inserted into the two constraints, eqs. (8)–(9), then two relations for λ_u and λ_v are obtained.

$$\left[\frac{\partial^2\lambda_u}{\partial t^2} + \frac{1}{\gamma}\frac{\partial^2\lambda_u}{\partial x^2} - f^2\lambda_u\right] + \frac{1}{\gamma}\frac{\partial^2\lambda_v}{\partial x\,\partial y} - 2f\frac{\partial\lambda_v}{\partial t} + E_u = 0 \tag{14}$$

$$\frac{1}{\gamma}\frac{\partial^2\lambda_u}{\partial x\,\partial y} + 2f\frac{\partial\lambda_u}{\partial t} + \left[\frac{\partial^2\lambda_v}{\partial t^2} + \frac{1}{\gamma}\frac{\partial^2\lambda_v}{\partial y^2} - f^2\lambda_v\right] + E_v = 0 \tag{15}$$

which with the boundary conditions

$$\begin{aligned} \lambda_u = \lambda_v = 0 &: \text{ initial and final times} \\ \lambda_u = 0 &: x \text{ boundaries} \\ \lambda_v = 0 &: y \text{ boundaries} \end{aligned} \tag{16}$$

form a closed problem. Thus eqs. (14)–(16) are solved to obtain λ_u and λ_v, and then the adjustments can be computed from (11)–(13).

3. Details of adjustment process

3.1 *Discretization of adjustment equations*

As was mentioned in section 2, centered differences in space and time are used in the evaluation of the budget equations (3) and (4). Since relatively large adjustments to the geopotential are expected, an effort is made in this study to avoid inconsistent finite differencing errors in ϕ such as those described in Sasaki et al. (1979).

This is done by offsetting λ_u λ_v (and thus, E_u and E_v) in space from the points where the winds and geopotentials are defined. Fig. 1b shows the arrangement; λ_u and E_u are displaced one half grid in the x-direction, λ_v and E_v are displaced one half grid in the y-direction.

Define the operators:

$$\overline{(\quad)}^k \equiv 1/2\,|(\quad)_{k+1/2} + (\quad)_{k-1/2}|,$$

$$\delta_k(\quad) \equiv \frac{1}{\Delta k}|(\quad)_{k+1/2} - (\quad)_{k-1/2}|,$$

and

$$\Delta_k(\quad) \equiv \delta_k(\overline{\quad})^k,$$

where Δ_k represents one grid interval. Using these relations, the residuals are computed from

$$\Delta_t \tilde{u}^{-x} + \tilde{u}^{-x}\,\delta_x \tilde{u} + \tilde{v}^{-x}\,\Delta_y \tilde{u}^{-x} + \tilde{\omega}^{-x}\,\Delta_p \tilde{u}^{-x} - f\tilde{v}^{-x} + \delta_x \tilde{\phi} = E_u \tag{17}$$

$$\Delta_t \tilde{v}^{-y} + \tilde{u}^{-y}\,\Delta_x \tilde{v}^{-y} + \tilde{v}^{-y}\,\delta_y \tilde{v} + \tilde{\omega}^{-y}\,\Delta_p \tilde{v}^{-y} + f\tilde{u}^{-y} + \delta_y \tilde{\phi} = E_v \tag{18}$$

while the constraints become

$$\Delta_t v^{-x} - f v^{-x} + \delta_y \phi + E_u = 0 \tag{19}$$

$$\Delta_t v^{-y} + f u^{-y} + \delta_y \phi + E_v = 0 \tag{20}$$

and the adjustment relations become

$$u = \Delta_t \lambda_u^{-x} - f\lambda_v^{-y} \tag{21}$$

$$v = \Delta_t \lambda_v^{-y} + f\lambda_u^{-x} \tag{22}$$

$$\phi = \frac{1}{\gamma}|\delta_x \lambda_u + \delta_y \lambda_v| \tag{23}$$

$$\left[\delta_t \delta_t \lambda_u + \frac{1}{\gamma}\delta_x \delta_x \lambda_u - f^2 \lambda_u\right] + \frac{1}{\gamma}\delta_x \delta_y \lambda_v - 2f\Delta_t \lambda_v + E_u = 0 \tag{24}$$

$$\left[\delta_t \delta_t \lambda_v + \frac{1}{\gamma}\delta_y \delta_y \lambda_v - f^2 \lambda_v\right] + \frac{1}{\gamma}\delta_x \delta_y \lambda_u + 2f\Delta_t \lambda_u + E_v = 0. \tag{25}$$

3.2 *Iterative procedures*

There are two levels of iteration in the adjustment process. The first involves the solution of eqs. (24)–(25) while the second involves a treatment of the non-linear advection terms in the momentum equations in much the same fashion as was done in LB. Rather than combining eqs. (24)–(25) into one equation of very high order, this study seeks to solve the two lower-order equations concurrently. Note that the bracketed terms in those equations are elliptic in nature; thus the method used to solve these equations separates the elliptic terms from the rest, while it treats the remaining terms as forcing. The results from one equation are then used in the forcing terms of the other. This method does converge, although the rate of convergence depends on the smoothness of the initial forcing (E_u, E_v, since λ_u and λ_v are initially zero) and the nature of the boundary conditions. For the fields encountered in this work, the solution process typically required 4 to 8 iterations. A direct elliptic equation solver (POIS) developed by Swarztrauber and Sweet (1975) is the main element in this process.

Once the adjustments have been computed from a given set of residuals (E_u, E_v), a new set of residuals may then be computed through the use of eqs. (17)–(18). Excepting the vertical derivative, all $(\tilde{\ })$ quantities are replaced by $(\quad)_a$ quantities. After the first iteration, residuals computed in this manner are measures solely of the adjusted fields' departures from the nonlinear portion of the momentum constraints. This can be demonstrated with the residuals obtained after the ith iteration: ($E_u^{(i)}$, $E_v^{(i)}$). Manipulation of eqs. (3)–(9) yields

$$\begin{aligned} E_u^{(1)} &= \mathbf{V}_a^{(1)} \cdot \nabla u_a^{(1)} - \tilde{\mathbf{V}} \cdot \nabla u \\ E_v^{(1)} &= \mathbf{V}_a^{(1)} \cdot \nabla_a^{(1)} - \tilde{\mathbf{V}} \cdot \nabla v \end{aligned} \tag{26}$$

or, in general

$$\begin{aligned} E_u^{(i)} &= \mathbf{V}_a^{(i)} \cdot \nabla u_a^{(i)} - \mathbf{V}_a^{(i-1)} \cdot \nabla u_a^{(i-1)} \\ E_{v(i)} &= \mathbf{V}_a^{(i)} \cdot \nabla v_a^{(i)} - \mathbf{V}_a^{(i-1)} \cdot \nabla v_a^{(i-1)} \end{aligned} \tag{27}$$

This is the same iteration procedure used for the horizontal advection terms by LB.

Although the iteration of the nonlinear terms was rapidly convergent using surface data in LB, the process is less well behaved in this study. The main source of difficulty arises in regions of strong velocity gradients, where there exist small scale, large amplitude horizontal advections of momentum. In these areas, the adjustments tend to enhance

the small-scale structure in a manner reminiscent of nonlinear instability in numerical modelling, i.e. the small-scale features continually intensified causing the whole process to diverge. To reduce the impact of the large advection terms, the LB method is modified by the application of a nine-point spatial smoother (cf. Shapiro, 1970) just prior to the iteration process. Such a smoother sharply filters out $2\Delta x$ scale structure.

It should be stressed that the adjustment procedure presented in this paper does not employ a vertical iteration. Since the basic adjustment process is constrained only in (x,y,t) "slabs", there is no reason to assume that an iterative process in the vertical would be convergent. Thus, in this study, $\partial u/\partial p$ and $\partial v/\partial p$ are held fixed to the initial data; the adjustments at different levels interact via the updating of ω alone.

4. Case Studies of 22 May 1966 and 8 June 1966

4.1 *Case description*

The synoptic features of the pre-storm period during 8 June 1966 have been discussed in LB. For the sake of comparison, Fig. 2 shows the synoptic patterns of 8 June 1966 and 22 May 1966 at 850 mb taken from data gathered by National Weather Service rawinsondes launched at 06.00 CST. As one can see in the figures, the early morning features are similar in the neighbourhood of the NSSL mesonetwork (delineated by the polygon on each map). After 12 hours (not shown), the May pattern became much weaker with the wave structure over Texas and Oklahoma disappearing altogether.

The development of the surface patterns of moisture and temperature for the two cases is shown in Fig. 3. In both cases, strong gradients of temperature and moisture developed during the day, with the gradient in the NSSL mesonetwork becoming stronger in the May case. The sharp moisture gradient or dryline in the May case was studied by Schaefer (1974a,b) in his work on the structure and dynamics of drylines. Coincident with the strong moisture gradient in each case was a wind-shift line (cf. Fig. 4a in LB for the June case) which moved very little during the 3 hour (14.00–17.00 CST) analysis period used in this study. It was along these wind-shift lines that storms either formed (June) or were expected to form (May).

Bloom (1980) has a detailed comparison of the thermodynamic structure of the two cases, obtained from the NSSL mesoscale rawinsonde data. Briefly, the May case had a very moist but shallow layer capped by a strong inversion; the June case had a less moist but somewhat deeper layer capped by a weaker inversion.

4.2 *Momentum budget residuals*

The interpolated data for the two cases are put into equations (17)–(18) to generate initial or "input" residuals. Representative patterns of the two input residual fields E_u and E_v, at 850 mb and 16.00 CST, are displayed in Figs. 4a,c (May) and 5a,c (June). Note that the residual of 200×10^{-5} m s^{-2} would correspond to an error of 7 m s^{-1} in the change of a wind component over a period of an hour if concentrated solely in the time tendency. The input residuals in this study have magnitudes as large as $600–700 \times 10^{-5}$ m s^{-2} at the upper levels; thus there appears to be a considerable number of dynamical inconsistencies in the interpolated data sets.

The following is a summary of a detailed examination of the input residuals and their components:

(i) Time by time, level by level, for both cases the structure of the residual fields generally resemble the associated height gradient (HG) patterns. Frequently, the major HG extrema have an associated extremum in a residual field. For those points, the magnitude of HG is greater than the value of the residual.

(ii) Often, secondary extrema in the residual fields have no counterpart in the HG patterns. At those points, the magnitude of the residual is often greater than any of the other terms in the budget (i.e. all the terms in eqs. (17) or (18) are additive). Time tendency and horizontal advection are more important at those points than the Coriolis force or vertical advection.

(iii) There is a very general, although not monotonic, trend for the residuals to increase with height. This trend generally follows a trend for HG to increase with height.

(iv) Both cases are generally similar, both in the

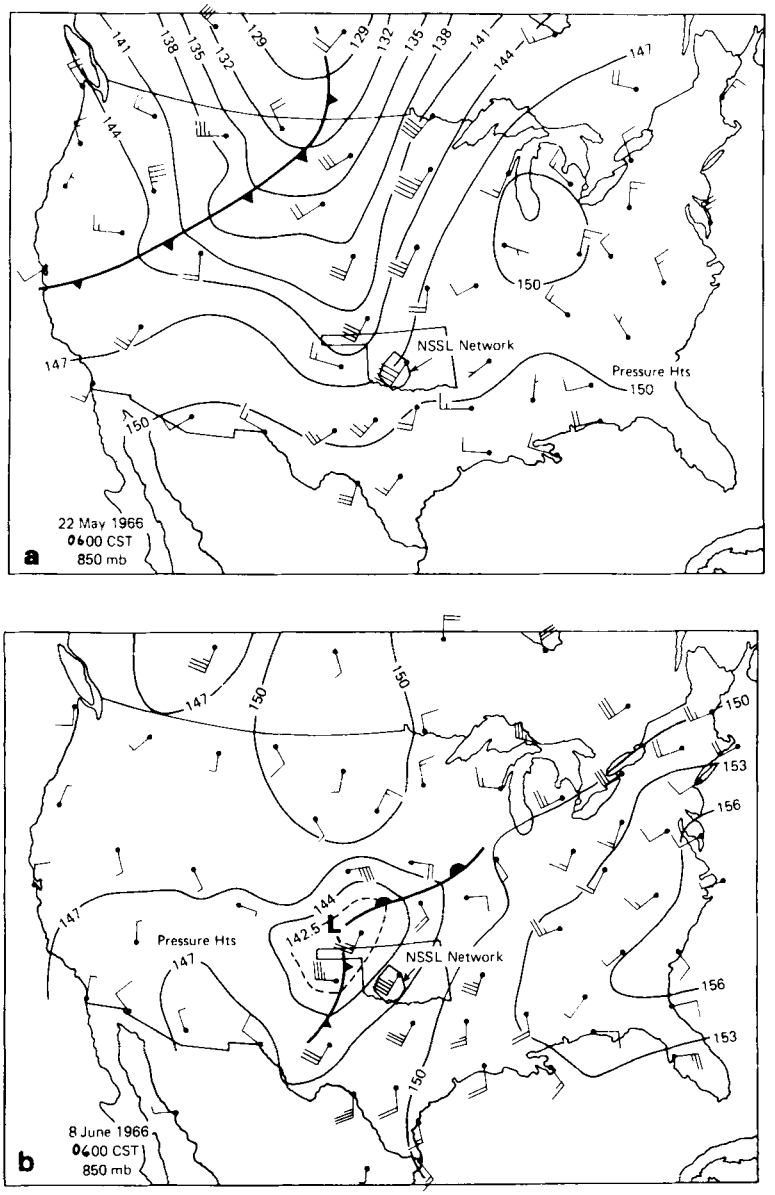

Fig. 2. Synoptic charts showing the significant weather patterns at 850 mb at 0600 CST. A full Wind barb means 5 m s^{-1} and the pressure heights are in decameters. Also shown is an outline of the NSSL rawinsonde network for (a) 22 May 1966, (b) 8 June 1966.

size of the input residuals and in the overall details of the momentum budget. There are no preferred locations for the residual extrema; they occur both on horizontal boundaries and in the interior (as can be seen in Figs. 4–5). The main feature distinguishing June from May is a huge anomaly in HG in the June case in the upper levels (700–400 mb) during the early times (14.00–15.00 CST). This feature is responsible for residuals of 600–700 $\times$ 10^{-5} m s^{-2} which are larger than the residuals at any

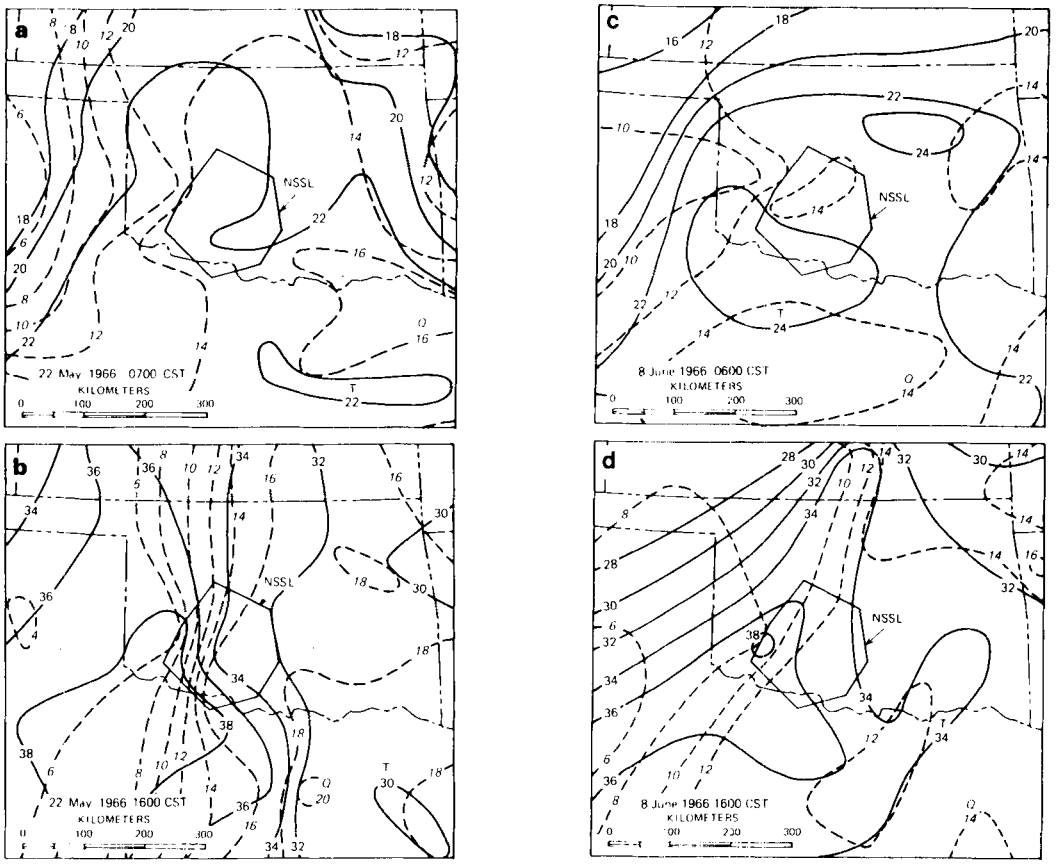

Fig. 3. Surface data analyses which show the development of the surface fields of temperature (°C, solid contours) and mixing ratio (g kg $^{-1}$ dashed lines). Area shown includes the state of Oklahoma and northern Texas; also indicated (as in Fig. 2) is the outline of the NSSL network. (a) 22 May 1966 0700 CST, (b) 22 May 1966 1600 CST, (c) 8 June 1966 0600 CST, (d) 8 June 1966 1600 CST.

other time (or those for May) by a factor of two or three.

These considerations confirm Fankhauser's caveat concerning mesoscale-derived geopotentials. The large HG in (iv) is located near COR (Cordell) in Fig. 1a. However an examination of the 14.00 CST sounding from that site uncovered nothing noteworthy.

4.3 *Data adjustment*

The adjustment process is applied to a 3-hour period (14.00–17.00 CST) from the interpolated data for each case. Figs. 4 and 5 show that the adjustments reduce the residuals significantly; however there remain some notable departures from zero in the adjusted residuals due to the approximate treatment of the advection terms. Although nonzero, the adjusted residuals are typically one to two orders of magnitude smaller than the input residuals. Thus the adjusted fields do satisfy the momentum constraints to a much greater extent than do the input fields.

A more detailed view of the adjustment process is presented in Fig. 6, which shows the RMS differences (computed using all interior x-y-t points at each level) between input and output for the three wind components and geopotential for May and June, respectively. The geopotential adjustments are systematically larger for the June case, which is another indication that there is some problem with the 8 June 1966 data set. Comparing Figs. 6a and 6b with the rawinsonde speed errors in

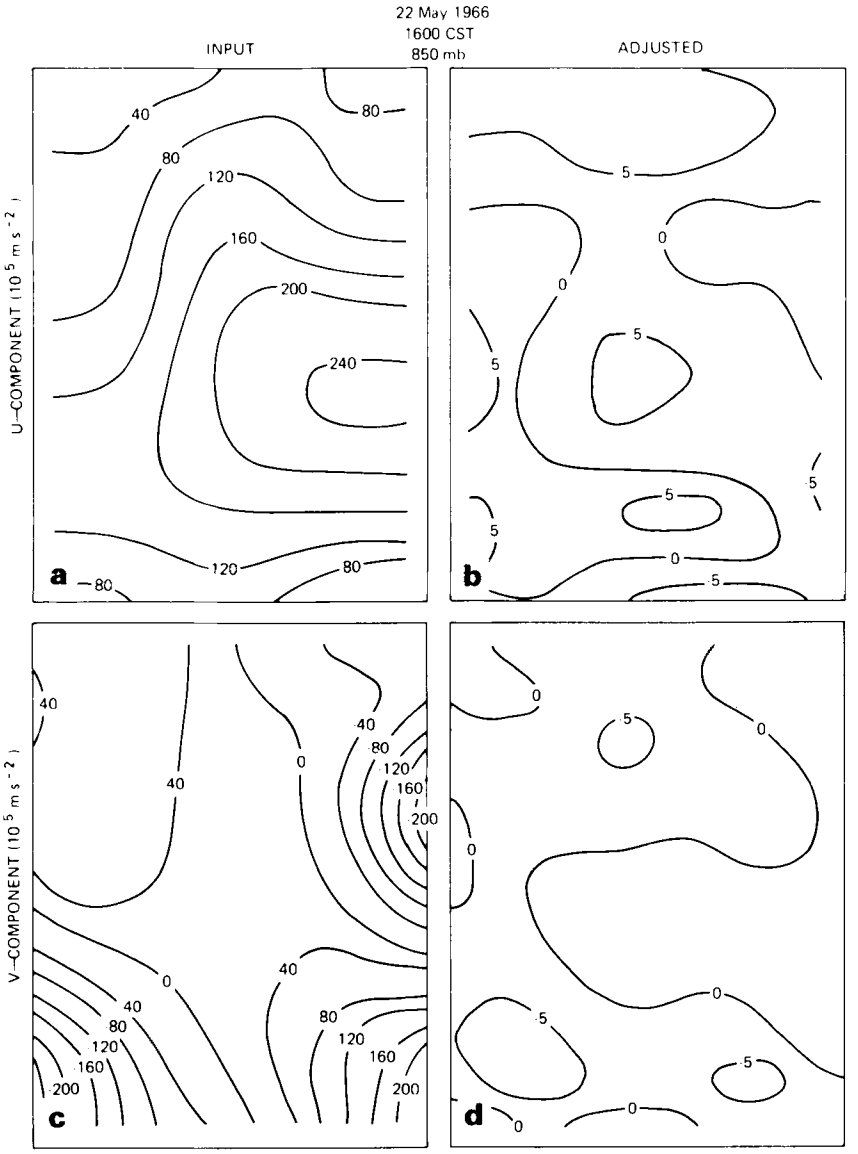

Fig. 4. Momentum budget residuals for 22 May 1966 at 850 mb and 1600 CST. (a) Input U, (b) adjusted U, (c) input V, (d) adjusted V. (Note, units have dimension of the time tendency of wind speed.)

Table 1, one finds the May and June RMS wind speed adjustments at 700 mb and 500 mb to be in rough agreement with observational error. At 850 mb and lower, both cases have RMS wind speed adjustments exceeding twice the observational error estimates at all levels.

The large adjustments to the June geopotentials at the upper levels are consistent with the large values of the residuals previously described at those levels. Note that both cases also have large adjustments at the bottom-most levels; this appears to indicate that the inviscid momentum constraints are not wholly satisfactory for data adjustment at the lower levels. A more detailed adjustment

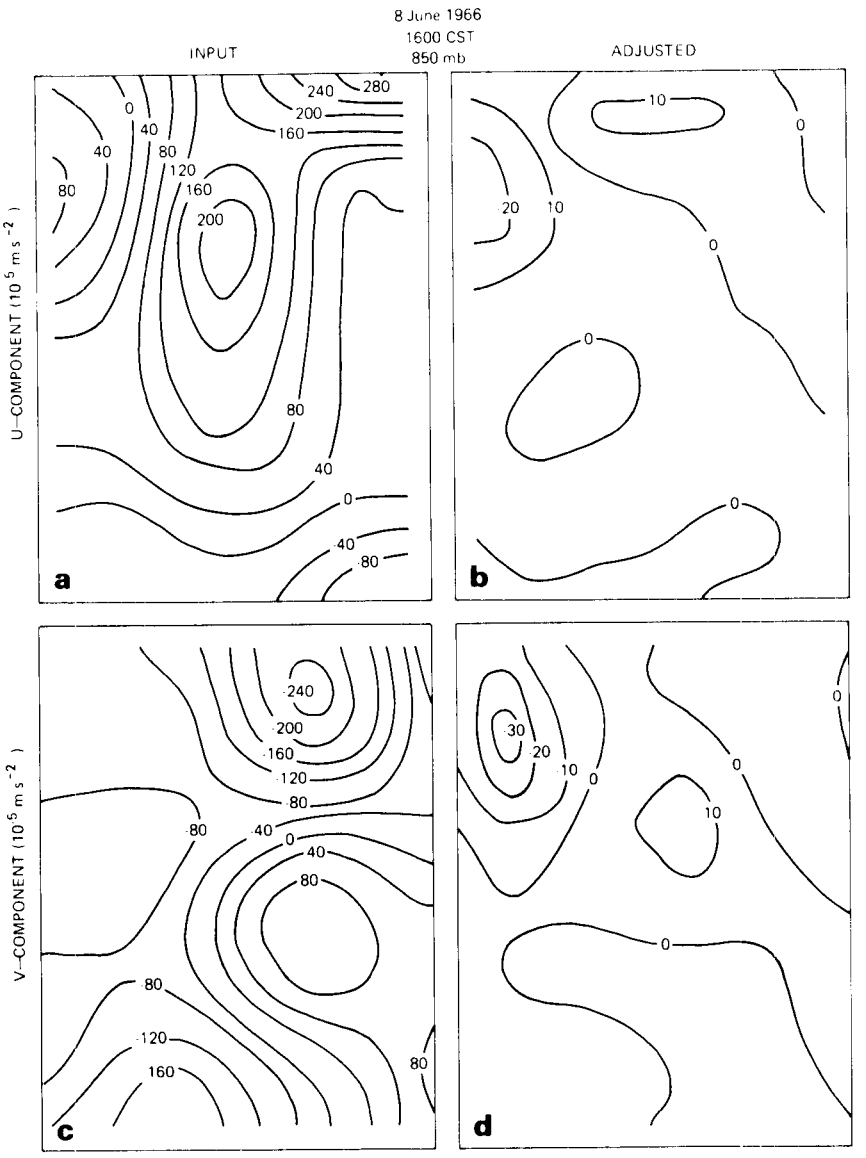

Fig. 5. Same as Fig. 4, for the 8 June 1966 case.

process should include some parameterization of the turbulent eddy stresses in the planetary boundary layer.

Fig. 7 shows how the adjustment process affects the vertical profiles of vertical velocity at selected gridpoints (the profiles are chosen at the points nearest to particular NSSL stations; refer to Fig. 1a for the location of each profile). The influence of the smoothing step in the adjustment process is clearly evident in the adjusted profiles. However, the adjustments involve more than smoothing alone, the adjustments display considerable horizontal variability. Finally, the adjusted vertical profiles have vertical structures which are similar to or smoother than the profiles from the input fields. Thus the lack of a vertical constraint in this adjustment process does not seem to lead to a noisier adjusted structure.

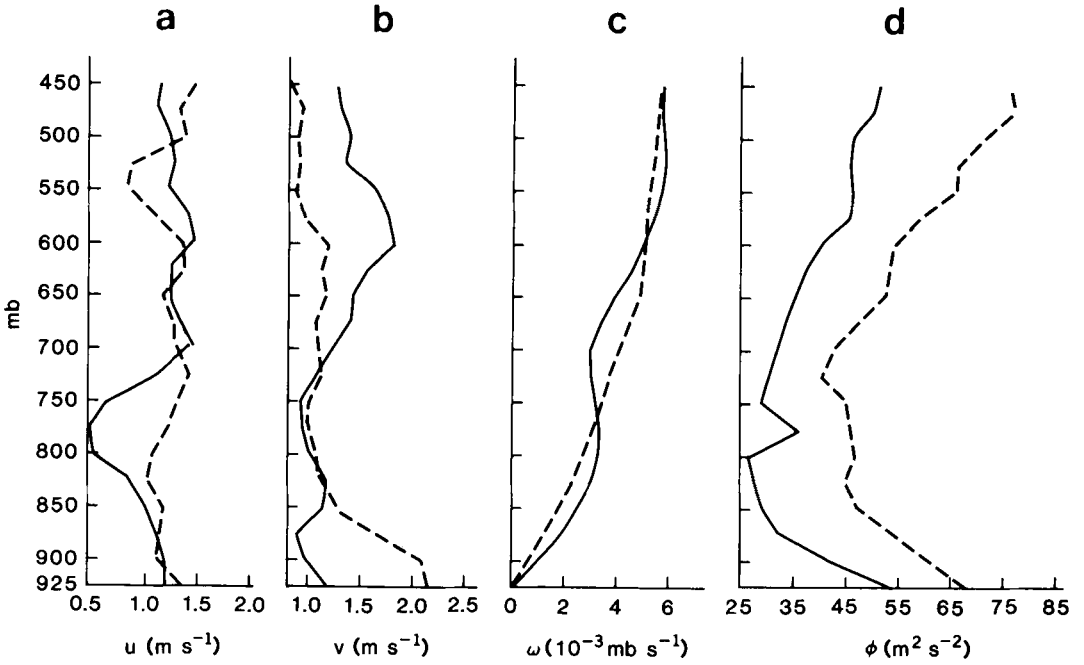

Fig. 6. Vertical profiles of the RMS adjustments. Solid lines are for 22 May 1966, dashed lines are for 8 June 1966. (a) RMS U adjustments, (b) RMS V adjustments, (c) RMS ω adjustments, (d) RMS ϕ adjustments.

A striking aspect of the adjustment process is displayed in Fig. 8, which shows horizontal sections of vertical velocity at 850 mb at 16.30 CST for both cases. Whereas the input patterns for the two cases are quite similar, the magnitudes of the adjusted May vertical velocities are substantially reduced in comparison to the adjusted June vertical velocities. The adjusted fields appear to be more in keeping with the events that occurred in the two cases: the June case had storms while the May case did not. A close examination of the May input winds found that the preponderance of the convergence responsible for the large input lifting maximum is due to the wind at one station, COR, whereas the June input lifting maximum can be traced to the convergence of wind over several stations. It thus appears that a characteristic of this adjustment process, in addition to an overall smoothing, is that grid points near aberrant observations receive larger adjustments consistent with the dynamical structure in space and time.

5. Discussion and conclusions

There have been many budget studies in which extensive physical interpretations have been made of residual terms. One of the main points of this research is that such residuals should be treated with caution, since in reality they represent both unresolved physical processes and analysis error. If one can correlate a pattern of residuals with an alternate source of data (satellite pictures, radar echoes, surface observations, etc.), then one can have a degree of confidence that those residuals may indeed be useful for physical investigations. However, as shown in section 4 of this paper, there may arise situations when the budget residuals do not have any obvious physical meaning. In those cases it seems reasonable to treat such residuals as indicators of analysis inaccuracies. Thus the primary goal of this research is diagnostic in nature: the development of an adjustment process for mesoscale rawinsonde data which produces fields with greatly reduced residuals.

Beyond the use of adjusted mesoscale analyses in purely diagnostic studies, it is reasonable to consider their use as initial fields in mesoscale forecast models. Since the adjusted analyses satisfy momentum constraints, gross imbalances due to analysis inaccuracies should be reduced, and in this sense the fields are initialized. It was the elimination of imbalances in the operational analyses of

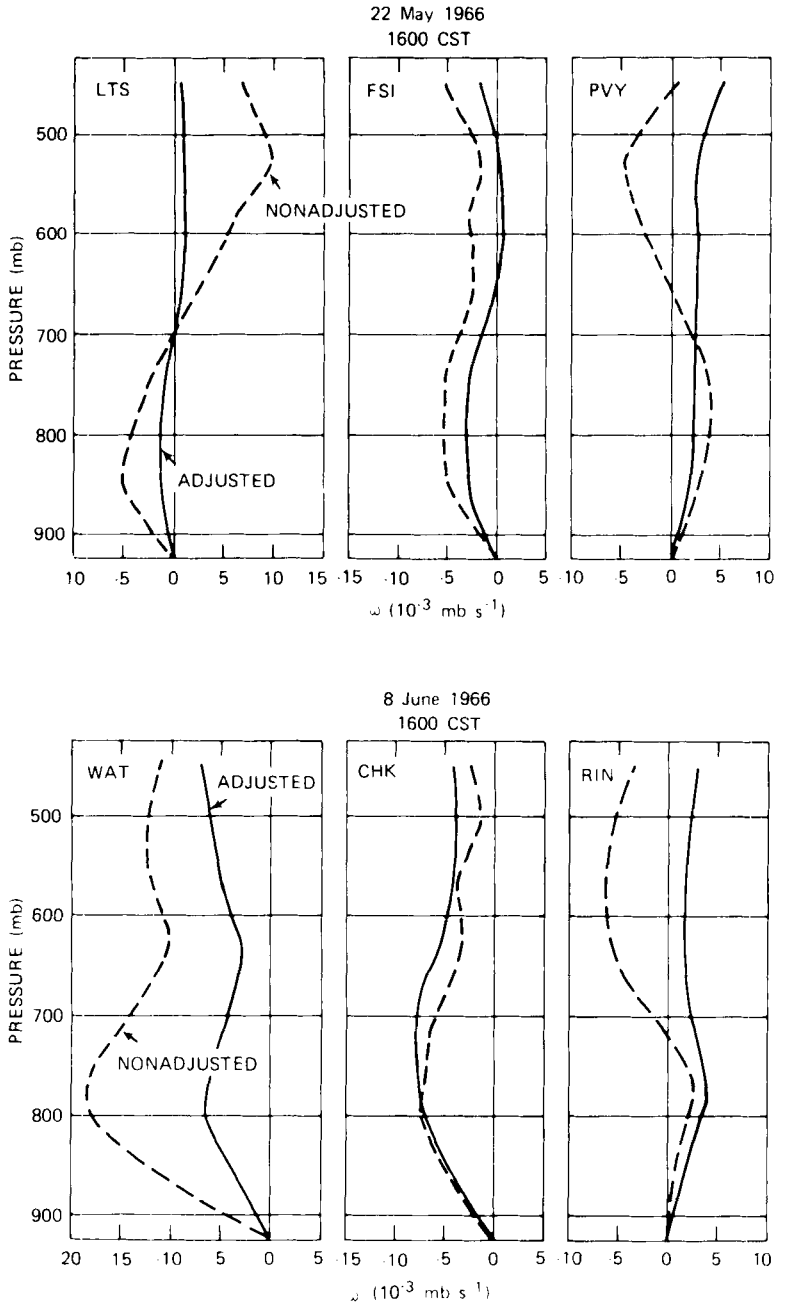

Fig. 7. Vertical profiles of ω at the fine-mesh gridpoints nearest the indicated station (see Fig. 1a) at 1600 CST; top: 22 May 1966, bottom: 8 June 1966.

global data sets that motivated the variational adjustment studies of Lewis (1972) and Lewis and Grayson (1972); their work involved the application of momentum constraints which used information from only one time. However, the use of time-dependent constraints in a variational adjust

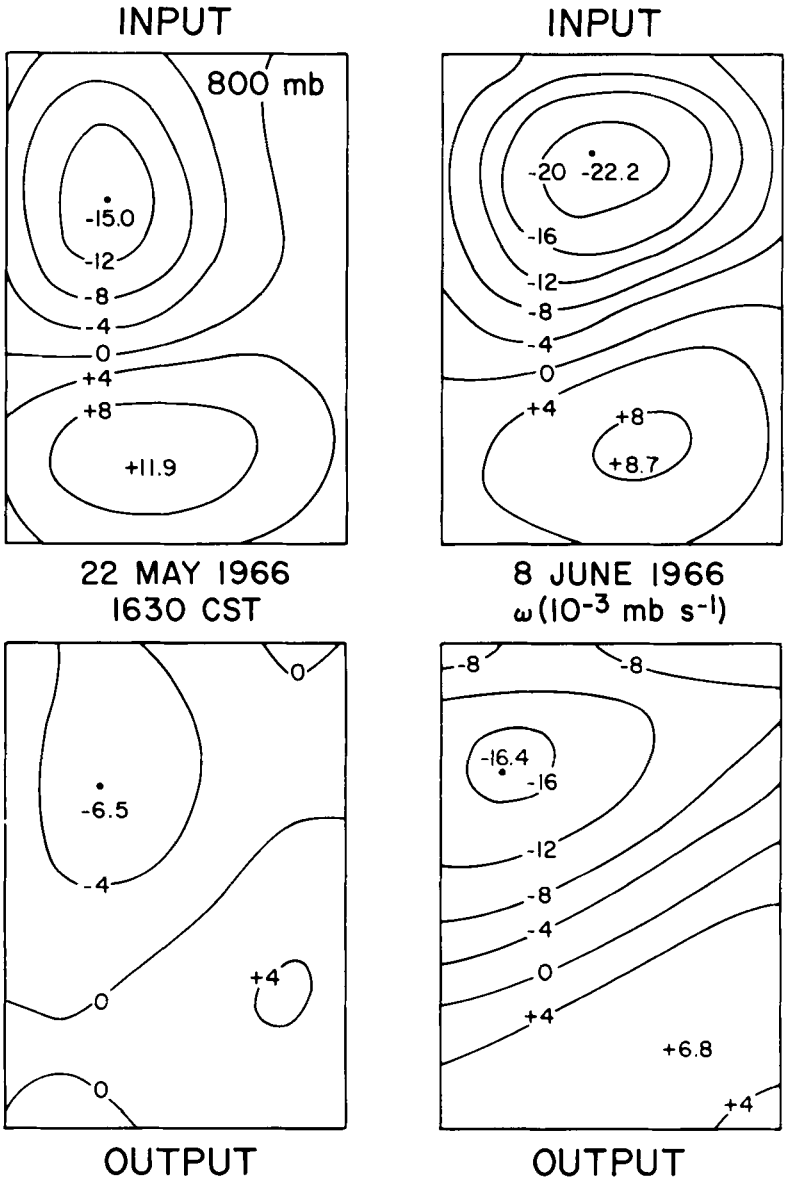

Fig. 8. Comparison of input and output (adjusted) ω at 800 mb and 1630 CST for both 22 May 1966 and 8 June 1966.

ment process appears to be incompatible with the initialization requirements of an operational mesoscale forecast model. The adjustment process described here requires a knowledge of all the data in advance, whereas an operational forecast model requires initialization as data become available. It is conceivable that a variational adjustment process with time-depend constraints could be used profitably in conjunction with a mesoscale forecast model in four-dimensional data assimilation studies.

The adjustment process described in this paper does produce mesoscale winds and geopotentials which are more dynamically consistent than the

original interpolated data. In addition, the vertical velocities computed kinematically from the adjusted winds are more in agreement with the nature of the weather in the two cases. Excepting the lowest levels, many of the RMS adjustments to the wind components and geopotential heights are 1–2 m s^{-1} and 3–6 m respectively, within the range of error for rawinsondes. At the lowest levels the RMS adjustments become consistently larger than the expected rawinsonde errors, suggesting that the choice of inviscid constraints is not wholly satisfactory near the surface boundary. Any future work in this area should consider some form of parameterization of turbulent stresses near the surface.

This research represents a first attempt to apply prognostic constraints to mesoscale rawinsonde data. A number of problems remain to be explored in this area. By computing temperatures hydrostatically from the adjusted geopotentials, one obtains temperature adjustments of the order of 1–2 °C, which are larger than the expected rawinsonde errors. It would appear that a more complete adjustment process would have to include some form of thermodynamic constraint; however, diabatic processes would make such an adjustment very difficult to apply if cumulus convection is present. Currently, the adjustments at each level are semi-indpendent of the adjustments at other levels. A more consistent adjustment process should couple the adjustments equally in the horizontal and the vertical directions. Finally, the details of the momentum constraints need further examination. As previously discussed, the inviscid assumption should be relaxed. Further work on the approximation of the advection terms may succeed in eliminating the current need of a smoothing step in the adjustment process. By smoothing the fields, this adjustment process may be removing some of the very important small scale features upon which subjective analysts focus attention (cf. Fujita, 1955 and Miller, 1972).

6. Acknowledgments

I am indebted to John M. Lewis for his help and encouragement during the course of this work. I am grateful to the following for their helpful comments on this manuscript: Y. Sasaki, T. Gal-Chen, W. Baker, J. McGinley and R. Hoffman. Support for this research was provided by the meteorological program of the Atmospheric Sciences Division of the National Science Foundation, Contract 74 21985ATM. In addition, computer resources for this work were provided by the University Research Board, University of Illinois at Urbana-Champaign. Portions of this paper were prepared while I was a post-doctoral fellow at the Cooperative Institute for Mesoscale Meteorological Studies (CIMMS), Norman, Oklahoma. The figures were drafted by J. Brothers, J. Kimpel (CIMMS), and L. Rumburg (NASA Goddard Space Flight Center). The manuscript was typed by J. Reckley (NASA Goddard Space Flight Center).

REFERENCES

Barnes, S. L., Henderson, J. H. and Ketchum, R. J. 1971. Rawinsonde observation and processing techniques at the National Severe Storm Laboratory. NOAA Tech. Memo. ERL NSSL-53, 246 pp.

Bloom, S. C. 1980. The objective analysis of pre-storm mesoscale rawinsonde data through the imposition of dynamical constraints. Ph.D. Thesis, Univ. of Illinois at Urbana-Champaign, Dept. of Physics, 109 pp.

Cline, A. K. 1973. Curve fitting using spline under tension. *Atmos. Technol. 3*, 60–65. National Center for Atmospheric Research, Boulder, Colorado.

Cressman, G. P. 1959. An operational objective analysis system. *Mon. Wea. Rev. 87*, 367–374.

Fankhauser, J. C. 1974. The derivation of consistent fields of wind and geopotential height from mesoscale rawinsonde data. *J. Appl. Meteorol. 13*, 637–646.

Fujita, T. 1955. Results of detailed synoptic studies of squall lines. *Tellus 7*, 405–436.

Kurihara, Y. 1961. Accuracy of winds—aloft data and estimation of error in numerical analysis of atmospheric motions. *J. Meteorol. Soc. Japan 39*, 333–345.

Lenhard, R. W. 1973. A revised assessment of radiosonde accuracy. *Bull. Amer. Meteorol. Soc. 54*, 691–693.

Lewis, J. M. 1972. The operational upper air analysis using the variational method. *Tellus 24*, 514–530.

Lewis, J. M. and Grayson, T. H. 1972. The adjustment of surface wind and pressure by Sasaki's variational matching technique. *J. Appl. Meteorol. 11*, 586–597.

Lewis, J. M. and Bloom, S. C. 1978. Incorporation of time continuity into sub-synoptic analysis by using dynamical constraints. *Tellus 30*, 496–516.

Miller, R. C. 1972. Notes on the analysis and severe storm forecasting procedures of the military weather warning center. U.S. Air Weather Service Tech. Report. No. 200, Kansas City, Missouri, 125 pp.

Ogura, Y. and Chen, Y. 1977. A life history of an intense mesoscale convective storm in Oklahoma. *J. Atmos. Sci. 34*, 1458–1476.

Sasaki, Y. 1958. An objective analysis based on the variational method. *J. Meteorol. Soc. Japan 36*, 77–88.

Sasaki, Y. 1969. Proposed inclusion of time variation terms, observational and theoretical, in numerical variational objective analysis. *J. Meteorol. Soc. Japan 47*, 115–203.

Sasaki, Y. 1970. Some basic formalisms in numerical variational analysis. *Mon. Wea. Rev. 98*, 875–883.

Sasaki, Y. K., Ray, P. S., Goerss, J. S. and Solig, P. 1979. Inconsistent finite differencing errors in the variational adjustment of horizonal wind components. *J. Meteorol. Soc. Japan 57*, 88–92.

Schaefer, J. T. 1974a. A simulative model of dryline motion. *J. Atmos. Sci. 31*, 956–964.

Schaefer, J. T. 1974b. The life cycle of the dryline. *J. Appl. Meteorol. 13*, 444–449.

Schaefer, J. T. and Doswell III, C. A. 1979. On the interpolation of a vector field. *Mon. Wea. Rev. 107*, 458–476.

Schlatter, T. 1975. Some experiments with a multivariate statistical objective analysis scheme. *Mon. Wea. Rev. 103*, 246–257.

Shapiro, R. 1970. Smoothing, filtering, and boundary effects. *Rev. Geophys. Space Phys. 8*, 359–387.

Swartztrauber, P. and Sweet, R. 1975. Efficient FORTRAN subprograms for the solution of elliptic partial differential equations. National Center for Atmospheric Research Tech. Note. NCAR-TN/IA-109, 139 pp.

Thompson, P. D. 1969. Reduction of analysis error through constraints of dynamical consistency. *J. Appl. Meteorol. 8*, 738–742.

Wahba, G. and Wendelberger, J. 1980. Some new mathematical methods for variational analysis using splines and cross-validation. *Mon. Wea. Rev. 108*, 1122–1143.